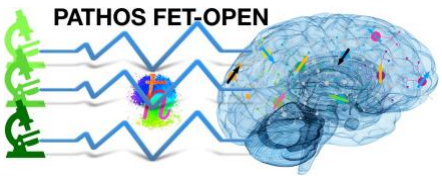

European Commission

PHOTONIC AND NANOMETRIC HIGH-SENSITIVITY BIO-SENSING

DELIVERABLE 3.6 [HUJI, M12]
REPORT ON OPTICAL CS IMAGING


PHOTONIC AND NANOMETRIC HIGH-SENSITIVITY BIO-SENSING

Compressive Sensing in NV Centers Report HUJI

John Howell

In collaboration with Nir Bar Gil's group, we have studied both theoretically and experimentally an adaptive compressed sensing technique for spatial magnetic sensing in Nitrogen Vacancy Centers. Using a highly overcomplete sparsifying basis we achieve compression ratios that range between 1.5 to 2.5. The aim is to achieve rapid characterization of the coarse magnetic field in an NV centers system.

I. INTRODUCTION

Compressed Sensing in recent years has emerged as a technique that allows determination of a signal even if the number of measurements is drastically sub-sampled compared to traditional techniques such as raster scanning. Successfully reconstructing a signal requires that the signal permits a sparse representation in some basis and that the measurements taken can be expressed as orthogonal, or at least incoherent, projections onto that sparsifying basis. If both of these are true, then by seeking a solution for the underlying vector that maximizes sparsity we can ensure that the signal is accurately reconstructed, even in the presence of noise. ([1], [2]) Due to the possibility of decreasing measurement time, cost, complexity, or some combination of all three, compressed sensing has found application in a wide variety of fields, including bio-sensing [3], Magnetic Resonance Imaging [4], LIDAR ([5], [6]), and quantum sensing and state tomography (two or three references here).

Furthermore, by dynamically adjusting our measurements and assumption of the underlying structure of the signal it is possible to work adaptively. By using information from previous guesses of a signal to not only improve the guess for a new measurement, but also decide how it might be best to sample. In such a way the number of required measurements to successfully reconstruct can be decreased further, not only decreasing the measurement time, but at least in certain cases, provide a better estimate of a sparse signal than traditional methods. ([7], [8])

Though early formulations of compressed sensing and their corresponding proofs of accuracy and convergence often assume that the sparse-representation of an underlying signal is in an orthonormal basis, for instance in a fourier or wavelet basis, increased attention is now being paid to compressed sensing techniques where the sparse representation is neither normalized or orthogonal, and may even be highly overcomplete. ([9], [10])

Here we present a technique that combines both of these elements, we use an adaptive procedure with a highly overcomplete sparse basis and apply it to the problem of magnetic sensing using Nitrogen-Vacancy (NV) centers in diamond. ([11], need way more references)

NV centers are known to be superb magnetic sensors. NV centers have unique features that make them stand out in the world of magnetic measurements, they provide a quantitative, vectorial measurement, with high magnetic sensitivity and high spatial resolution, under ambient conditions. Magnetic sensing with NV's is possible in several measurement schemes, we have focused on exploiting adaptive compressive sensing for wide field imaging, when a full magnetic resonance measurement is needed. By using adaptive compressed sensing we would like to maintain

magnetic sensitivity while shortening measurement times and improving bandwidth.

We present the basic theory underlying the fluorescence lineshape and how it relates to the vectorial magnetic field and how this lineshape may be represented with an overcomplete but sparse basis. We explain how we exploit the structure of this basis, rooted in the physics of the NV centers, to design our application-specific adaptive compressed sensing technique. We follow by a description of the fluorescence imaging microscope we use to measure the magnetic field at each pixel as well as our results using the algorithm. Finally, limitations and possible improvements of the technique are discussed.

II. THEORY

The NV center is a point defect in the diamond lattice. It consists of a Nitrogen atom and a vacancy in an adjacent lattice site. In the diamond there are four crystallographic orientations possible for the NV, In an ensemble, all orientations are equally populated. The ground state of the NV is a spin triplet, where the $m_s = 0$ and $m_s = \pm 1$ have a zero field splitting of $2.87GHz$ due to spin-spin interactions. When applying a small magnetic field along the NV center's symmetry axis, the degeneracy of the $m_s = \pm 1$ is lifted due to Zeeman splitting, the shift is given by $\delta = m_s \gamma B_{||}$, where $\gamma = g\mu_B/h = 2.8MHz/G$ is the gyromagnetic ratio. Between the ground and excited triplet there is a zero phonon line of 637 nm, with a phonon sideband of 640-800 nm at room temperature. When the NV is optically excited from the ground to the excited states, there are two ways for it to decay. It can either cycle down directly, and radiatively, which is spin conserving or decay in a non radiative way, through the singlet state, which isn't spin conserving. The probabilities and rates of these processes make it possible to polarize the spin state of the NV center and enable spin state fluorescent readout since fluorescence intensity corresponds with spin state. Using this effect by employing Optically Detected Magnetic Resonance (ODMR) one can measure the resonances of the NV by sweeping over microwave (MW) frequency (ODMR, ref).

ODMR is the easiest way to measure magnetic field with NV's (ref), since the resonance frequencies are proportional to the external magnetic field. Four NV orientation correspond to 8 resonances, which is the full ODMR spectra The setup is a wide field, Epi-Illumination microscope, where an area of the diamond is imaged onto a sCMOS camera, green laser is used to excite the NV's, and manipulation is done with a MW antenna. In this scheme we receive a full ODMR spectra, per pixel. From that, a three axes magnetic image can be extracted. In what follows we present the technique over the averaged image, and not per pixel.

A. Adaptive Compressed Sensing

In our experiment the bias magnetic field determines the window over which we expect frequencies to occur. Define this set of M frequencies $\{\nu_j\}_{j=1}^{M}$ at which we may measure and define the set of frequencies $\{\nu_k\}_{k=1}^{N}$ as those locations where we allow for the possibility that a resonance is present. Note that it is not necessary, and in practice not the case that any $\nu_j = \nu_k$, only that they share the window over which resonances actually occur in our system. We can write the total lineshape $A(\nu)$ at frequency ν_j as

$$\begin{aligned} A(\nu_j) &= \left(\frac{(\frac{2}{\pi\sigma_k})}{1 + \frac{4(\nu_j - \nu_k)^2}{\sigma_k^2}} \right) a_k \\ &= L_{jk} a_k \end{aligned}$$

Where we have cast this into matrix form and define $\mathbf{L} \doteq \{L_{jk}\}$ the normalized lorentzian lineshape centered at a location ν_k with width σ_k measured at frequency ν_j and $\mathbf{a}$ as the vector of amplitudes of the lorentzians at each frequency ν_k. Note that we expect only a few of the coefficients (two if we had a single NV center with no noise), in $\mathbf{a}$ to be non-zero, i.e. $\mathbf{a}$ is *sparse*.

For this experiment we consider projections made up of not individual frequencies. Instead we apply one set of microwave frequencies $\{\nu_j^+\}$, measure the reference and signal powers then choose a different set of frequencies $\{\nu_j^-\}$ according and subtract the result as a single projection. The choice of which frequencies we apply and which are positive or negative for each projection can be summarized in an M-column sampling matrix $\mathbf{S}$ who's elements are $\{1, 0, -1\}$. Each row corresponds to a single projection with ±1 entries corresponding to the random frequencies chosen for the sets $\{\nu_j^{\pm}\}$ respectively and zeros if that microwave frequency was not chosen at all. In this experiment we considered two separate situations, one where we apply one microwave frequency for the $\{\nu_j^{\pm}\}$ so in each projection there are two non-zero entries in each row of $\mathbf{S}$ and applying two microwave frequencies at a time so that there are four non-zero entries in each row. Our measured data $\mathbf{y}$ we can then represent as

$$\mathbf{y} = \mathbf{SLa}.$$

This now has all the elements we need for a compressed sensing reconstruction.

We adopt an adaptive strategy where the reconstruction at each step informs where we sample, weighting our choice of where non-zero elements occur in each new row of $\mathbf{S}$, as well as where we guess the basis support of the underlying function $A(\nu)$ lies, equivalent to updating $\mathbf{L}$.

Our procedure is as follows: we first sample at a number of frequencies across *all* ν_j, not just the resonance window and gain an estimate of the average reference power $\bar{\mathrm{P}}_r$.

Once these peak locations have converged, we change $\mathbf{L}$ to have support at exactly each one of the converged locations and now allow the width to vary. If the peaks and widths are still consistent the algorithm terminates returning the best estimate of the reconstruction, otherwise a new projection is measured and a reconstruction is attempted again with the new widths. The pseudo-code for this procedure can be found in Alg. 1.

[H] Estimate of where Lorentzian Peaks Occur Measure user-defined (small) number of initial projections at randomly chosen frequencies Get initial estimate of mean reference power and peak locations fit has NOT converged choose random frequencies within window we know resonances should appear measure a new projection at those frequencies get new reconstruction estimate and peak locations 8 peaks have converged update basis matrix $\mathbf{L}$ at the converged locations but with a range of widths get new reconstruction estimate and peak locations Reconstruction has converged OR max number of measurements reached return current reconstruction as best estimate Update basis matrix $\mathbf{L}$ to a few MHz window around each peak with the updated widths.

Adaptive Reconstruction We use total variation minimization, specifically the algorithm provided by the TVAL3 ([12]) package in MATLAB, to reconstruct our 1D signal at each reconstruction step. We use the anisotropic version with positivity constraints:

$$\min_a \sum_i \|D_i a\|_1 \text{ s.t. } \mathbf{a} \geq 0 \text{ and } \mathbf{SLa} = y$$

Where $D_i a$ is the discrete gradient of $\mathbf{a}$.

As long as the underlying noise level is low enough we achieve effective compression ratios that range from 1.5 to 2.5. The compression ratio depends on the underlying noise level, desired accuracy, and the effect of random sampling in a given acquisition of the experiment. We only consider a set of 180 sample frequencies and keep our guessed basis of relatively low dimension ($\approx$ 1000 at the largest) so that each reconstruction is only a few milliseconds. A representative reconstruction is depicted in Fig. 1. The parameters of most interest, the peak locations, in the reconstruction provide an excellent estimate of the raster scan locations even in the presence of a small amount of noise. If the contrast of the peaks is well above the noise level, which for our system was primarily limited by power fluctuations of the 532 nm pump laser, the adaptive algorithm terminates successfully with both high probability and with a high compression ratio. To better characterize the algorithm we run 150 trials, saving the reconstruction estimate at each reconstruction step in each trial. We compare the peak locations found in the reconstruction.

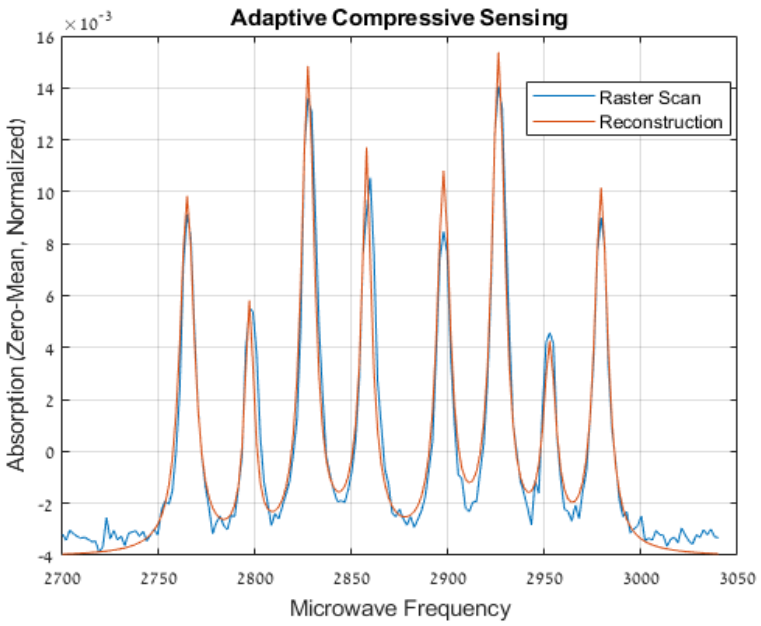

FIG. 1. A typical adaptively reconstructed signal and a corresponding raster scan. Here the compression ratio is ~ 1.73 and we only apply one microwave frequency at a time.

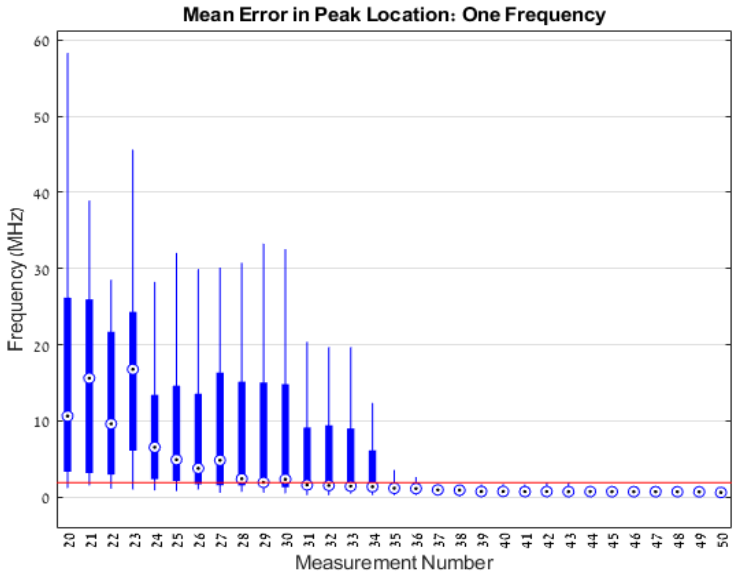

FIG. 2. We run the experiment 150 times, for each measurement number (projection) in each run of an experiment we save the reconstruction and compare the found peak locations with the peak locations from fitting eight lorentzians to a raster scan. The red horizontal line marks the frequency spacing ≈ 1.9 MHz of the 180 sample frequencies. The means are marked with circles, solid bar contains 50% of the trials and thin bars mark the upper 75% and lower 25% quintile about the mean.

DISCUSSION

We still need to quantify if the compressive sensing is faster than a pure raster scan in terms of frequency uncertainty in the low measurement limits.

---

[1] E J Candes and M B Wakin, "An introduction to compressive sampling," IEEE Signal Process. Mag. **25**, 21–30 (2008).

[2] Marco F Duarte and Yonina C Eldar, "Structured compressed sensing: From theory to applications," IEEE Signal Process. Mag. (2011), arXiv:1106.6224 [cs.IT].

[3] Darren Craven, Brian McGinley, Liam Kilmartin, Martin Glavin, and Edward Jones, "Compressed sensing for bioelectric signals: a review," IEEE J Biomed Health Inform **19**, 529–540 (2015).

[4] Oren N Jaspan, Roman Fleysher, and Michael L Lipton, "Compressed sensing MRI: a review of the clinical literature," Br. J. Radiol. **88**, 20150487 (2015).

[5] Gregory A Howland, Daniel J Lum, Matthew R Ware, and John C Howell, "Photon counting compressive depth mapping," Opt. Express **21**, 23822–23837 (2013).

[6] Yoni Sher, Lior Cohen, Daniel Istrati, and Hagai S Eisenberg, "Low intensity LiDAR using depth aware compressive sensing and a photon number resolving detector," in *Imaging and Applied Optics 2019 (COSI, IS, MATH, pcAOP)* (Optical Society of America, 2019) p. JW2A.6.

[7] M L Malloy and R D Nowak, "Near-Optimal adaptive compressed sensing," IEEE Trans. Inf. Theory **60**, 4001–4012 (2014).

[8] A Soni and J Haupt, "Efficient adaptive compressive sensing using sparse hierarchical learned dictionaries," in *2011 Conference Record of the Forty Fifth Asilomar Conference on Signals, Systems and Computers (ASILOMAR)* (2011) pp. 1250–1254.

[9] M Sadeghi, M Babaie-Zadeh, and C Jutten, "Learning overcomplete dictionaries based on Atom-by-Atom updating," IEEE Trans. Signal Process. **62**, 883–891 (2014).

[10] Emmanuel J Candès, Yonina C Eldar, Deanna Needell, and Paige Randall, "Compressed sensing with coherent and redundant dictionaries," Appl. Comput. Harmon. Anal. **31**, 59–73 (2011).

[11] Linh My Pham, *Magnetic Field Sensing with Nitrogen-Vacancy Color Centers in Diamond*, Ph.D. thesis, Harvard (2013).

[12] Chengbo Li, *Compressive Sensing for 3D Data Processing Tasks: Applications, Models and Algorithms*, Ph.D. thesis, Rice University (2012).